6 Huminiecki L, Gorn M, Suchting S et al. Magic roundabout is a new member of the roundabout receptor family that is endothelial specific and expressed at sites of active angiogenesis. Genomics 2002;79:547–552.
7 Park KW, Morrison CM, Sorensen LK et al. Robo4 is a vascular-specific receptor that inhibits endothelial migration. Dev Biol 2003;261:251–267.
8 Forsberg EC, Prohaska SS, Katzman S et al. Differential expression of novel potential regulators in hematopoietic stem cells. PLoS Genet 2005;1:e28.
9 Zhang J, Niu C, Ye L et al. Identification of the haematopoietic stem cell niche and control of the niche size. Nature 2003;425:836–841.
10 Calvi LM, Adams GB, Weibrecht KW et al. Osteoblastic cells regulate the haematopoietic stem cell niche. Nature 2003;425:841–846.
11 Goodell MA, Brose K, Paradis G et al. Isolation and functional properties of murine hematopoietic stem cells that are replicating in vivo. J Exp Med 1996;183:1797–1806.
12 Goodell MA, Rosenzweig M, Kim H et al. Dye efflux studies suggest that hematopoietic stem cells expressing low or undetectable levels of CD34 antigen exist in multiple species. Nat Med 1997;3:1337–1345.
13 Arai F, Hirao A, Ohmura M et al. Tie2/angiopoietin-1 signaling regulates hematopoietic stem cell quiescence in the bone marrow niche. Cell 2004;118:149–161.
14 Tulin EE, Onoda N, Maeda M et al. A novel secreted form of immune suppressor factor with high homology to vacuolar ATPases identified by a forward genetic approach of functional screening based on cell proliferation. J Biol Chem 2001;276:27519–27526.
15 Nakano T, Kodama H, Honjo T. Generation of lymphohematopoietic cells from embryonic stem cells in culture. Science 1994;265:1098–1101.
16 Nakajima H, Shibata F, Fukuchi Y et al. Immune suppressor factor confers stromal cell line with enhanced supporting activity for hematopoietic stem cells. Biochem Biophys Res Commun 2006;340:35–42.
17 Ema H, Morita Y, Yamazaki S et al. Adult mouse hematopoietic stem cells: Purification and single-cell assays. Nat Protoc 2006;1:2979–2987.
18 Kitamura T, Koshino Y, Shibata F et al. Retrovirus-mediated gene transfer and expression cloning: Powerful tools in functional genomics. Exp Hematol 2003;31:1007–1014.
19 Morita S, Kojima T, Kitamura T. Plat-E: An efficient and stable system for transient packaging of retroviruses. Gene Ther 2000;7:1063–1066.
20 Ueno H, Sakita-Ishikawa M, Morikawa Y et al. A stromal cell-derived membrane protein that supports hematopoietic stem cells. Nat Immunol 2003;4:457–463.
21 Tamura S, Morikawa Y, Hisaoka T et al. Expression of mKirre, a mammalian homolog of *Drosophila* kirre, in the developing and adult mouse brain. Neuroscience 2005;133:615–624.
22 Goolsby J, Marty MC, Heletz D et al. Hematopoietic progenitors express neural genes. Proc Natl Acad Sci U S A 2003;100:14926–14931.
23 Klein R. Eph/ephrin signaling in morphogenesis, neural development and plasticity. Curr Opin Cell Biol 2004;16:580–589.
24 Augustin HG, Reiss Y. EphB receptors and ephrinB ligands: Regulators of vascular assembly and homeostasis. Cell Tissue Res 2003; 314:25–31.
25 Suenobu S, Takakura N, Inada T et al. A role of EphB4 receptor and its ligand, ephrin-B2, in erythropoiesis. Biochem Biophys Res Commun 2002;293:1124–1131.
26 Silvestri F, Banavali S, Baccarani M et al. The CD34 hemopoietic progenitor cell associated antigen: Biology and clinical applications. Haematologica 1992;77:265–273.
27 Shalaby F, Rossant J, Yamaguchi TP et al. Failure of blood-island formation and vasculogenesis in Flk-1-deficient mice. Nature 1995;376: 62–66.
28 Ziegler BL, Valtieri M, Porada GA et al. KDR receptor: A key marker defining hematopoietic stem cells. Science 1999;285:1553–1558.
29 Rhee J, Mahfooz NS, Arregui C et al. Activation of the repulsive receptor Roundabout inhibits N-cadherin-mediated cell adhesion. Nat Cell Biol 2002;4:798–805.
30 Zhou S, Schuetz JD, Bunting KD et al. The ABC transporter Bcrp1/ABCG2 is expressed in a wide variety of stem cells and is a molecular determinant of the side-population phenotype. Nat Med 2001;7: 1028–1034.
31 Zhou S, Morris JJ, Barnes Y et al. Bcrp1 gene expression is required for normal numbers of side population stem cells in mice, and confers relative protection to mitoxantrone in hematopoietic cells in vivo. Proc Natl Acad Sci U S A 2002;99:12339–12344.
32 Morita Y, Ema H, Yamazaki S et al. Non-side-population hematopoietic stem cells in mouse bone marrow. Blood 2006;108:2850–2856.

See www.StemCells.com for supporting information available online.

Original Communications

Diameter of splenic vein is a risk factor for portal or splenic vein thrombosis after laparoscopic splenectomy

Katsuki Danno, MD,[a] Masataka Ikeda, MD, PhD,[a] Mitsugu Sekimoto, MD, PhD,[a] Tomoyuki Sugimoto, PhD,[b] Ichiro Takemasa, MD, PhD,[a] Hirofumi Yamamoto, MD, PhD,[a] Yuichiro Doki, MD, PhD,[a] Morito Monden, MD, PhD,[a] *and* Masaki Mori, MD, PhD,[a] *Suita, Japan*

Background. *Splenomegaly is a risk factor for post-splenectomy portal or splenic vein thrombosis (PSVT) due to large splenic vein stump. The relationship between splenic vein diameter (SVD) and PSVT has not been established.*

Objectives. *To investigate whether SVD is a risk factor for PSVT.*

Methods. *Forty patients who underwent laparoscopic splenectomy were analyzed. Preoperative and postoperative enhanced helical computed tomographic scans were obtained in all patients, and subsequent follow-up was performed in patients with PSVT during anticoagulant therapy. SVDs at the junction of portal vein (PV) 2, 4, and 6 cm from the junction of PV were measured preoperatively and postoperatively. Multivariate analysis was performed using logistic regression model.*

Results. *PSVT was diagnosed in 52.5% (21/40) patients. Preoperative SVD was significantly larger in patients with PSVT than in those without PSVT. Seventy-two percent of patients (16/22) with PSVT in splenic veins with a diameter of >8 mm developed PSVT. Multivariate analysis identified preoperative SVD as a significant and independent determinant of PSVT. At a cutoff value of 8 mm, receiver operator characteristic analysis for prediction of PSVT provided an area under the curve of 0.8552 (95% CI 0.821–1.000).*

Conclusion. *Preoperative SVD is a risk factor for post-splenectomy PSVT. We recommend measurement of SVD preoperatively in patients elected to undergo splenectomy, and a close follow-up of patients with SVD greater than 8 mm. (Surgery 2009;145:457-64.)*

From the Departments of Surgery[a] and Bio-Medical Statistics,[b] Graduate School of Medicine, Osaka University, Suita, Japan

PORTAL OR SPLENIC VEIN THROMBOSIS (PSVT) is a serious but rare complication of elective splenectomy.[1,2] However, with the improvement in diagnostic modalities and increased interest in this disease entity, it is becoming apparent that the incidence of PSVT is greater than clinically appreciated.[3-6] Since the clinical manifestations of PSVT are unspecific and most of the patients with radiologically detected PSVT are asymptomatic, diagnostic work-up, prophylaxis, and treatment for PSVT remain to be established.[7]

Accepted for publication June 23, 2008.

Reprint requests: Masataka Ikeda, MD, PhD, Department of Surgery, Graduate School of Medicine, Osaka University, E2-2-2 Yamadaoka, Suita, Osaka 565-0871, Japan. E-mail: mikeda@gesurg.med.osaka-u.ac.jp.

0039-6060/$ - see front matter

doi:10.1016/j.surg.2008.06.030

PSVT occurs as a result of one or several prothrombotic disorders. These factors can be grouped into systemic and local factors.[8] After splenectomy, the systemic factors include postoperative hypercoagulable state and thrombocytosis, while local factors such as venous flow congestion at the stump of the splenic vein may promote thrombus generation.

From a clinical point of view, splenomegaly, thrombocytosis and myelodysplastic disease are recognized risk factors for PSVT.[9] Some authors recommended imaging surveillance for patients with these risk factors.[3,4,10] Splenomegaly is considered a risk factor, because a large stump of splenic vein causes blood turbulence, which in turn can result in a local increase in coagulability and enhanced thrombus formation.[2,4] Postoperative thrombocytosis may also have a direct impact on thrombus formation.[11] Some groups recommended ligation of the splenic vein at the junction of the inferior

mesenteric vein (IMV) to prevent blood stasis.[12] Therefore, the size of splenic vein stump after splenectomy may play a role as a local factor, however, the relationship between the size of splenic vein stump and PSVT has not been established.

Because splenomegaly is caused by a variety of conditions, eg, portal hypertension, hypersplenism, inflammatory reaction, and tumor growth, the weight of the spleen cannot simply represent the size of splenic vein stump. Prediction of spleen weight before operation is time consuming. We hypothesized that the diameter of the splenic vein is directly related to the hemodynamic changes in the portal venous system, excluding patients with portal hypertension, and thus can be a more easily measurable predictor for PSVT than spleen weight. Accordingly, postoperative splenic vein diameter (SVD) may represent the flow dynamics of portal venous system after splenectomy, which could provide information regarding treatment strategy.

The aims of this study were to evaluate the impact of preoperative SVD on PSVT after splenectomy, and to determine the relationship between postoperative SVD changes and treatment outcome using prospectively collected data.

PATIENTS AND METHODS

Patient population. Fifty-three consecutive elective splenectomies, including laparoscopic splenectomy (LS) (n = 41) and hand-assisted LS (HALS, n = 12), were performed between April 2001 and June 2007 at the Department of Surgery, Osaka University Medical Hospital. Before entry into the study, informed consent was obtained from all patients. The operative technique was performed as described previously.[13] Age of the patients, sex, indication for surgery, operating time, blood loss, platelet count before the operation and on a post-operative day (POD 7 ± 1), spleen weight, occurrence of PSVT, and postoperative complications were recorded prospectively. Of the 53 patients, 17 patients overlapped with patients reported in our previous study.[13] Five patients (LS:4, HALS:1) were excluded from this analysis because of hypersensitivity to the intravenous contrast media used in helical computed tomography (CT), renal dysfunction, or anomalies of the portal venous system. Another group of 8 patients (LS:0, HALS:8) with portal hypertension due to liver cirrhosis was excluded from this analysis because the high portal vein pressure could influence SVD. Thus, the study population consisted of 40 patients (LS:37, HALS:3). These consisted of 26 patients with idiopathic thrombocytopenic purpura, 7 with malignant lymphoma, 2 with splenic lymphangioma/hemangioma, 2 with hereditary spherocytosis, 1 with autoimmune hemolytic anemia, 1 with Evans syndrome, and 1 with splenic cyst (Table I).

Detection and diagnosis of PSVT. All 40 patients underwent preoperative and postoperative helical CT with intravenous contrast media. Imaging analysis was performed prospectively before operation, and after splenectomy between POD 3 and POD 11 (median 6.0 POD). Detection of PSVT was based on the criteria defined previously.[3,13] In brief, PSVT was diagnosed when an unenhanced region was detected in a dilated splenoportal system, which was otherwise free of any abnormality in the preoperative CT. PSVT was classified into 5 types according to the location of the thrombus.[13] Distal splenic vein thrombosis (dSVT) was defined as thrombosis located in the splenic vein distal to the junction of IMV. Thrombi between the portal vein and IMV were classified as proximal SVT (pSVT). Total splenic vein thrombosis (tSVT) (pSVT+dSVT) was defined as thrombosis involving the entire splenic vein. When IMV was directed towards the superior mesenteric vein (SMV), splenic vein thrombosis was defined as dSVT. Thrombosis in SMV, intra- and extra-hepatic portal vein was classified as SMVT, iPVT, and ePVT, respectively.

Intermittent pneumatic foot pump was used for perioperative prophylaxis of deep venous thrombosis until full ambulation, but no anticoagulant was used for all patients.

Measurement of SVD. SVD was measured on helical CT scan transaxial images using Aquarious NET server (TeraRecon Inc., San Mateo, CA) at 4 different locations; at the junction of splenic vein and PV (Fig 1, *A*, location *a*), 2 cm from the junction (Fig 1, *A*, location *b*), 4 cm from the junction (Fig 1, *A*, location *c*), and 6 cm from the junction (Fig 1, *A*, location *d*). SVD was measured on at least two or three sequential enlarged CT images (× 2–× 3) at all 4 locations, and the largest diameter was selected for analysis.

Statistical analysis. Continuous data are expressed as median and range, unless otherwise specified. Statistical analysis was performed using the Chi-square test or the Fisher exact test for categorical data and the Mann-Whitney U test for nonparametric continuous data. The Wilcoxon signed rank test was used to compare preoperative and postoperative or post-treatment SVD. The relationships between clinical features and the incidence of PSVT were examined using logistic regression models in the single-variate and multivariate analyses. The above statistical analyses were completed using StatView 5.0J software

Table I. Comparison of clinical features of patients with or without portal or splenic vein thrombosis

	No PSVT (n = 19)	*PSVT (n = 21)*	P *value*†
Age (years)*	56, 17–74	37, 18–73	.233
Sex (M:F)	7:12	5:16	.369
BMI (kg/m^2)*	22.6, 17.9–30.3	22.1, 18.2–24.3	.364
Operating time (min)*	135, 65–200	115, 66–358	.291
Blood loss (ml)*	40, 6–180	20, 10–160	.156
Platelet count: preoperative ($\times 10^4/\mu L$)*	8.8, 1.4–21.9	9.7, 2.6–27.4	.218
Platelet count: POD 7±1 ($\times 10^4/\mu L$)*	19.5, 0.7–52.4	28.8, 2.9–75.7	.06
Spleen weight (g)*	122, 11–608	220.5, 61–2315 ($n = 20$)	.028
Surgical procedure (LS:HALS)	19:0	3:18	.087
Indication for surgery			
Benign:Malignant	16:3	17:4	.787
Idiopathic thrombocytopenic purpura	15	11	
Splenic lymphangioma/hemangioma	0	2	
Hereditary spherocytosis	0	2	
Autoimmune hemolytic anemia	0	1	
Evans syndrome	0	1	
Splenic cyst	1	0	
Malignant lymphoma	3	4	

BMI, Body mass index.
*Data are median and range, or number of patients.
†By Chi-square test or Fisher exact test for categorical data and Mann-Whitney *U* test for nonparametric continuous data.

(SAS Institute Inc., Cary, NC). A *P* value of <.05 was considered statistically significant. The usefulness of individual prognostic values was estimated using the analysis of receiver operating characteristic (ROC) curves, which were constructed using the R statistical software from http://www.r-project.org.

RESULTS

Incidence of PSVT and comparison of perioperative factors. PSVT was diagnosed in 52.5% (21/40) patients. The number of patients and thrombus location were: 5 patients with both iPVT and dSVT, 6 with iPVT only, 3 with both iPVT and tSVT, 2 with tSVT only, 3 with dSVT only, and 2 with ePVT, iPVT, and tSVT. In our 40-case series, 4 patients were symptomatic: 4 had fever greater than 38°C, and 2 had abdominal pain of unknown cause.

There were no significant differences between patients with and without PSVT in terms of age, sex, BMI, operating time, blood loss, and platelet count (preoperative and POD 7 ± 1), surgical procedure, indication for surgery (Table I). However, the weight of the resected spleen was significantly greater in patients with PSVT than those without PSVT ($P = .028$).

Preoperative SVD was then compared between patients with and without PSVT. As shown in Fig 2, preoperative SVD measured at all locations in patients with PSVT was significantly greater than in patients without PSVT. Nine of 11 (82%) patients with preoperative SVD at location *b* of more than 10 mm had PSVT. Furthermore, in patients with preoperative SVD of 8 to 10 mm, 6 to 8 mm, and <6 mm measured at location *b*, the incidence of PSVT was 64% (7/11), 43% (6/14), and 0% (0/4), respectively. In patients with preoperative SVD of more than 10 mm at locations *a*, *b*, *c*, and *d*, the incidence of PSVT was 100% (6/6), 82% (9/11), 100% (8/8), and 89% (8/9), respectively.

Comparison of postoperative and post-treatment SVD. In order to compare the flow dynamics of portal venous system after splenectomy, we compared postoperative SVD in patients without PSVT and post-treatment SVD in patients with PSVT after recanalization. Of the 21 patients with PSVT, 4 received intravenous infusion or subcutaneous heparin (adjusted individually with the aim of 1.5- to 2-fold prolongation of the pretreatment activated partial thromboplastin time) followed by oral anticoagulation with warfarin, while 16 patients received only warfarin. The dose of warfarin was adjusted to achieve an international normalized ratio (INR) between 1.5 and 2.0. The last patient had dSVT only and did not receive any anticoagulation. Unresolved dSVT was found in 6 patients in spite of anticoagulation for 3 to 6 months; however, all other PSVTs resolved during the same period. One patient had short splenic vein stump after splenectomy; SVD in this patient could not be measured at locations *c* and *d*. The median preoperative SVD at locations *a*, *b*, *c*, and *d* in patients who

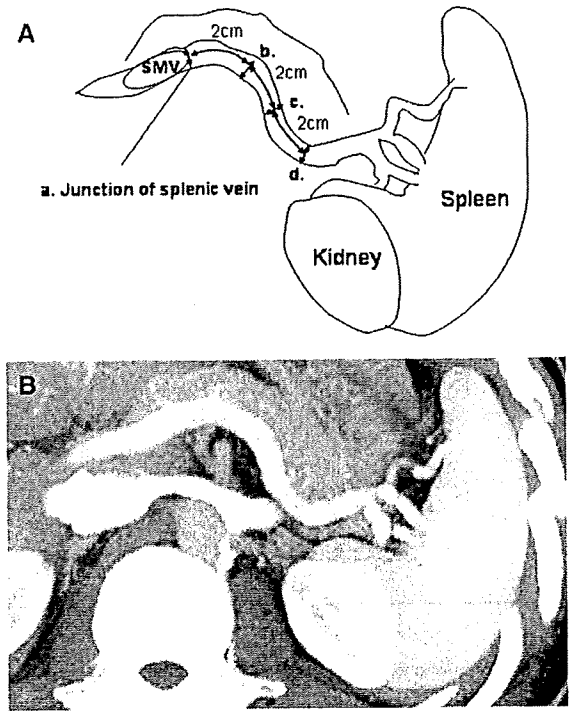

Fig 1. Measurement locations of splenic vein diameter and corresponding computed tomographic image. (*A*) Splenic vein diameter (SVD) was measured in the transaxial images of computed tomography (CT) at the junction of portal vein (*a*), and 2 cm (*b*), 4 cm (*c*), and 6 cm (*d*) from the junction of portal vein. (*B*) Representative image of CT for measurement of SVD.

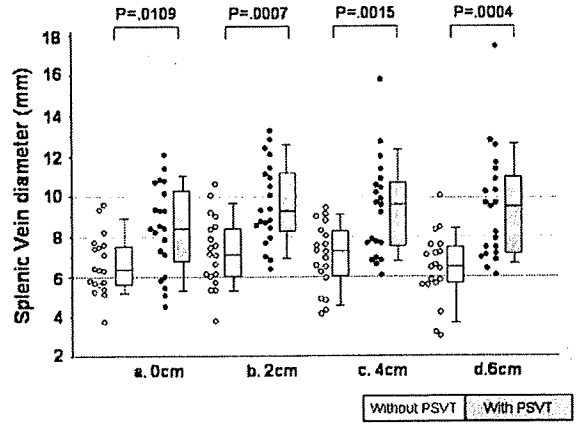

Fig 2. Box-and-whisker plots of preoperative SVD in patients with and without portal or splenic vein thrombosis (PSVT). Symbols: values of individual patients, boxes: group data. Open symbols and boxes: patients without PSVT, Gray symbols and boxes: patients with PSVT. In these plots, lines within the boxes represent median values; the upper and lower lines of the boxes represent the 25th and 75th percentiles, respectively; and the upper and lower bars outside the boxes represent the 90th and 10th percentiles, respectively. Statistical analysis was performed using the Mann-Whitney *U* test.

did not develop PSVT was 6.4, 7.2, 7.3, and 6.5 mm, respectively (Table II). The median postoperative SVD at the same locations after operation decreased to 6.1, 6.2, 5.9, and 5.7 mm, respectively, and these changes except for SVD at location *a* were significant (Table II). In patients with PSVT, the respective preoperative values were 8.4, 9.3, 9.6, and 9.5 mm, which decreased to 5.2, 5.5, 4.9, and 3.9 mm, respectively, after treatment (Table II). The reduction in SVD was significant for all 4 locations.

Fig 3 shows the rate of reduction of SVD following splenectomy. The median SVD reduction rate in patients without PSVT was less than 25% at each of the 4 locations, while that in patients with PSVT was significantly greater at each of the 4 locations. Differences in SVD following splenectomy were compatible with the results of rate of reduction (data not shown).

Multivariate analysis. Multiple logistic regression analysis was performed to summarize the development of PSVT and the multivariable associations with variables potentially considered as independent risk factors for PSVT following splenectomy. Ten factors identified by univariate analysis (listed in Table I) and preoperative SVD values measured at 4 different locations from the junction of PV were considered candidate covariates that could be included in the multivariate analysis. The type of surgical procedure (LS vs HALS) was excluded from the multivariate analysis, because information on surgical procedure is covered or carried by that of spleen weight in this study, ie, HALS was performed in patients with spleen weight greater than 650 g while patients less than 650 g underwent LS. Each value of preoperative SVD measured at 4 locations (SVD *a*, *b*, *c*, and *d*) was included separately in the analysis, since the 4 measurements had quite similar information to each other and, in particular, averaging them in the multivariate analysis is inappropriate due to problems of multi-colinearity as well as interpretability in multivariate fitting. Based on these considerations, the 10 factors: age, sex, BMI, malignant versus benign, operating time, blood loss, platelet counts before operation and at POD 7, spleen weight and a preoperative SVD value measured at 1 of the 4 locations, to sufficiently describe differences in characteristics of patients and/or confounders, were included in the multivariate analysis.

Table III shows the results of multiple logistic regression analysis when such analysis included one

Table II. Changes in splenic vein diameter after surgery

	No PSVT (n = *20*)			*PSVT* (n = *21*)		
Location	*Before surgery*	*After surgery*	P *value**	*Before surgery*	*After treatment*	P *value**
a	6.4, 5.1–9.6	6.1, 4.2–7.8	.0663	8.4, 4.5–12.1	5.2, 3.6–8.2 (*n* = 20)	<.0001
b	7.2, 3.8–10.6	6.2, 4.0–8.5	.0150	9.3, 6.4–13.3	5.5, 2.0–7.9 (*n* = 20)	<.0001
c	7.3, 4.2–9.5	5.9, 4.1–7.9	.0004	9.6, 6.2–15.9	4.9, 2.2–7.5 (*n* = 19)	<.0001
d	6.5, 3.3–10.0	5.7, 2.0–7.8	.0095	9.5, 6.1–17.7	3.9, 1.4–5.4 (*n* = 15)	<.0001

Data are median, range (mm).
*By Mann-Whitney *U* test.

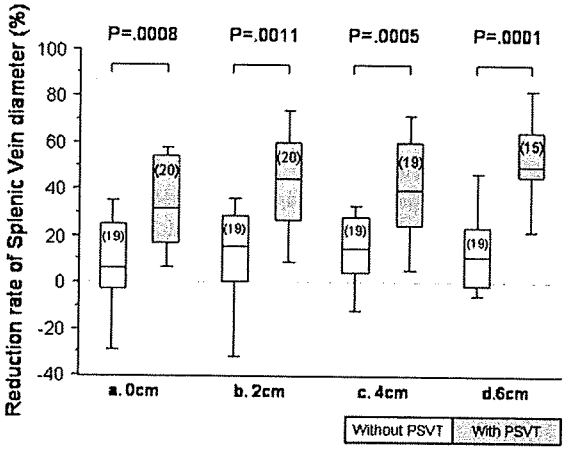

Fig 3. Box-and-whisker plots of the rate of reduction of SVD in patients with and without PSVT. Reduction rate (%) = (preoperative SVD − postoperative SVD)/preoperative SVD × 100. Numbers in parentheses indicate the number of SVDs measured. Symbols: values of individual patients, boxes: group data. Open symbols and boxes: patients without PSVT. Gray symbols and boxes: patients with PSVT. In these plots, lines within the boxes represent median values; the upper and lower lines of the boxes represent the 25th and 75th percentiles, respectively; and the upper and lower bars outside the boxes represent the 90th and 10th percentiles, respectively. Statistical analysis was performed using the Mann-Whitney *U* test.

preoperative SVD value measured at any of the 4 locations. Preoperative SVD measured at location *b* was identified as the only significant determinant of PSVT ($P = .014$), while the other factors were not ($P > .05$) under the sample size of this study. In addition, the results of multivariate analysis using any of the preoperative SVD measured at the other 3 locations also identified preoperative SVD as the only significant risk factor ($P = .022$, .004, and near 0 for SVD *a*, *c*, and *d*, respectively), while all the other factors did not achieve statistical significance. These results indicate that preoperative SVD, irrespective of the site of measurement, directly influenced the development of PSVT, while all other 9 factors, especially spleen weight, did not. To further explain the above findings, we included only two variables in the multiple logistic regression models: spleen weight and preoperative SVD values measured at the 4 locations (which were identified as significant factors in univariate analysis). The results of such analysis also identified each of the preoperative SVD value as significant determinant of PSVT ($P = .027$, .003, .007, and .0006 for SVD *a*, *b*, *c*, and *d*, respectively) but not spleen weight ($P = .456$, .643, .958, and .773, respectively).

Results of ROC analysis. Since multivariate analysis identified preoperative SVD value measured at each of the 4 locations as significant determinant of postoperative PSVT, we next analyzed the cutoff values of preoperative SVD that can best predict the development of PSVT by multiple logistic regression model that included preoperative SVD grouped at a cutoff value and the other 9 covariates used in the multivariate analysis. For such analysis, we used 8 mm as the cutoff value for preoperative SVD *b*, because it was found to be the best determination when searching the integer values (6, 7, 8, 9, 10, and 11 mm) with clinical convenience. As a risk estimate for the development of PSVT in preoperative SVD *b* grouped at the cutoff value of 8 mm, the adjusted odds ratio of patients with SVD ≥8 mm to those with <8 mm was 5.221 (95% confidence interval [95% CI] 1.017–33.46). Fig 4 shows the results of ROC analysis for prediction of PSVT, based on this logistic regression model, including preoperative SVD *b* grouped at a cutoff value of 8 mm. The AUC was 0.8552 (95% CI 0.821–1.000).

DISCUSSION

Splenomegaly is considered as a risk factor for PSVT after splenectomy.[6,9,10,12] A large stump of splenic vein tends to enhance thrombosis probably due to blood stasis and turbulence.[1,2] Although splenomegaly indirectly indicates splenic vein

Table III. Results of multivariate logistic regression analysis of post-splenectomy PSVT

	Estimate (log-OR)	*95% confidence interval*	P *value**
Age	0.0078	−0.047, 0.063	.781
Sex (M:0, F:1)	−0.0193	−2.858, 2.820	.989
BMI (kg/m^2)	−0.3075	−0.769, 0.154	.164
Malignant vs benign	−1.1937	−4.618, 2.231	.496
Operating time (min)	−0.0105	−0.034, 0.013	.374
Blood loss (ml)	−0.0006	−0.025, 0.024	.964
Platelet count: preoperative ($\times 10^4/\mu$L)	0.0075	−0.007, 0.022	.295
Platelet count: POD 7 ($\times 10^4/\mu$L)	0.0003	−0.005, 0.006	.916
SVD at location *b* (mm)	0.6280	0.052, 1.204	.013
Splenic weight	0.0029	−0.004, 0.010	.238

SVD, Splenic vein diameter.
*The relationships between the parameters and incidence of PSVT was examined by logistic regression models in the single-variate and multivariate analyses.

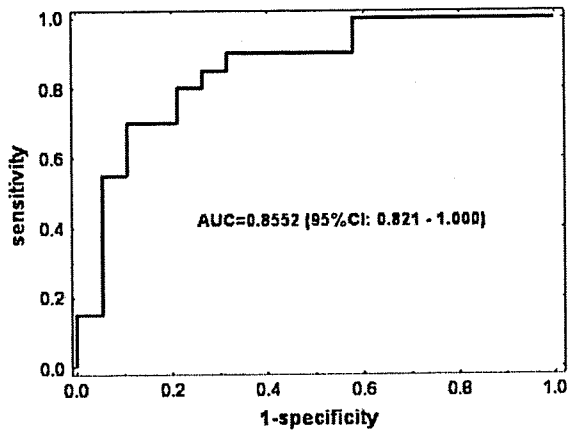

Fig 4. Receiver operator characteristic curve prediction of post-splenectomy PSVT using preoperative SVD value. Values for the area under the curve (AUC) and 95% confidence intervals are provided.

dilation, the direct relationship between SVD and post-splenectomy PSVT has rarely been studied. Possible reasons are (1) the majority of all retrospective analyses have been evaluated by ultrasonography and retrospective data collection was impossible, (2) measurement of SVD was not included in the prospective trials. Since we have been studying postsplenectomy PSVT with contrast helical CT, we were able to review and collect data of SVD pre- and postoperatively. Moreover, as we described in our previous study,[13] the usefulness of CT for the diagnosis of PSVT after splenectomy has been emphasized previously.[2-4,10] We prefer to perform CT rather than ultrasonography to detect PSVT, because it provides precise and objective information on PSVT for the entire portal venous system as well as on other lesions such as bowel edema and ascites. The drawbacks of CT are exposure to radiation and use of contrast material.

Our analysis demonstrated that preoperative SVD in patients who later developed PSVT was significantly larger than that of patients who did not develop PSVT irrespective of surgical treatment, and that the incidence of PSVT after laparoscopic splenectomy correlated with preoperative SVD. Especially, the incidence of PSVT in patients with preoperative SVD greater than 8 mm was very high. Multivariate analysis identified preoperative SVD, irrespective of the location of measurement, as a significant independent risk factor for PSVT. Because measurement of SVD is very simple and easy, preoperative SVD can be a very useful indicator in the prediction of post-splenectomy PSVT. We recommend measuring SVD preoperatively in patients elected to undergo splenectomy.

We found significant differences in preoperative SVD at all 4 locations. For practical purposes, SVD should be measured at about 2 cm distal from the PV junction, because it is visually easier to recognize this portion on transaxial CT images than other locations. Eguchi et al[14] demonstrated that SVD was significantly larger in patients with idiopathic portal hypertension (IPH) than in those with liver cirrhosis (16.2 vs 14.2 mm), and the incidence of PSVT was higher in patients with IPH than those with liver cirrhosis. Although their investigation was conducted in patients with portal hypertension, our results in patients with normal portal pressure are consistent with their data in terms of SVD and tendency for PSVT. They concluded that a decrease in blood flow in the portal vein might be associated with the development of PSVT in patients with IPH. De Cleva et al[15] also found low blood flow in portal veins of patients with PSVT after esophagogastric devascularization with splenectomy for

hepatosplenic infestation with *Schistosoma mansonia.* However, the difference in the reduction of portal flow was not significant between patients with and without PSVT (42 ± 16 vs 33 ± 30%). Since reduction in SVD correlates with reduction in portal or splenic vein blood flow, we speculate that the greater the reduction rate of SVD is, the greater the incidence of PSVT. Our data on the reduction rate of SVD clearly showed that the reduction rate of SVD in patients with PSVT was significantly greater than in patients without PSVT.

We also found that the reduction of the size of SVD in patients with PSVT were greater than those without PSVT. Since thrombosis exacerbates narrowing of the splenic vein, these results might not be the cause, but rather the effect of thrombosis. However, we have one possible explanation for that. After splenectomy, splenic vein flow is reduced, followed by a decrease in SVD. These changes enhance the development of PSVT. A marked decrease in splenic vein flow volume following splenectomy requires sufficient narrowing of the splenic vein in order to maintain splenic vein flow speed; otherwise, thrombosis develops in the splenic vein, leaving little space for drainage of decreased blood flow. Thus, a greater reduction rate of SVD and larger reduction in size was noted in patients with PSVT. On the other hand, moderate or mild decrease in splenic vein flow volume is not associated with narrowing of the splenic vein and hence protects against thrombosis. Our results that the reduction rate of SVD and reduction in size were smaller in patients without PSVT are consistent with this hypothesis.

Before the present study, many patients who underwent laparoscopic splenectomy had uneventful recovery without any treatment for PSVT. However, it was reported that progression of the thrombus to occlude the portal and mesenteric veins could cause acute hypertension in the splanchnic circulation and intestinal infarction, which negatively influences the outcome in these patients.[2] Accordingly, we believe that prevention of further thrombus propagation is vital, even in patients asymptomatic at the time of a diagnosis. Since we do not know the natural history of PSVT and there is no supporting evidence on no-treatment, we are in the situation that all PSVT would better be treated unless clinically contraindicated. We have recently reported that patients with total splenic vein thrombosis are more likely to develop clinical symptoms and are thus candidate for aggressive treatment.[16] Importantly, since CT can detect small thrombi, not all patients with PSVT detected by CT are symptomatic. Further research on patients with asymptomatic PSVT must be carried out.

In conclusion, preoperative SVD was identified as a significant independent determinant of post-splenectomy PSVT, with a calculated cutoff value of 8 mm. We currently perform pre- and post-operative CT routinely to detect PSVT. However, there are many issues to be answered. For example, should all patients be screened? Should asymptomatic PSVT be treated? Should prophylaxis be carried out for patients with greater SVD? We plan prospective studies to resolve such issues. Future prospective studies related to post-splenectomy PSVT need to include measurement of pre- and post-operative SVD to clarify these issues. Because hemodynamic changes in the portal system play pivotal role and can be influenced by pneumoperitoneum, measurement of splenic vein flow is also mandatory. Prospective investigation of post-splenectomy PSVT to evaluate these factors would answer questions on postoperative surveillance, efficacy of prophylaxis, and treatment of PSVT.

This study did not demonstrate the risk of laparoscopic surgery on post-splenectomy PSVT. Since pneumoperitoneum-associated hemodynamic changes and coagulation impairment have been postulated recently as etiologic factors for PSVT,[17-20] prospective randomized studies that compare the incidence of PSVT between laparoscopic and open splenectomy with similar patient background stratified by SVD are necessary.

In conclusion, preoperative SVD is a risk factor for post-splenectomy PSVT. We recommend measurement of SVD preoperatively in patients elected to undergo splenectomy. Patients with preoperative SVD greater than 8 mm should be closely monitored after splenectomy because they are at high risk for portal or splenic vein thrombosis.

REFERENCES

1. Gertsch P, Matthews J, Lerut J, Blumqart LH. Acute thrombosis of the splanchnic veins. Arch Surg 1993;128:341-5.
2. Rattner DW, Ellman L, Warshaw AL. Portal vein thrombosis after elective splenectomy. An underappreciated, potentially lethal syndrome. Arch Surg 1993;128:565-9.
3. Petit P, Bret PM, Atri M, Hreno A, Casola G, Gianfelice D. Splenic vein thrombosis after splenectomy: frequency and role of imaging. Radiology 1994;190:65-8.
4. Chaffanjon PC, Brichon PY, Ranchoup Y, Gressin R, Sotto JJ. Portal vein thrombosis following splenectomy for hematological disease: prospective study with Doppler color flow imaging. World J Surg 1998;22:1082-6.
5. Harris W, Marcaccio M. Incidence of portal vein thrombosis after laparoscopic splenectomy. Can J Surg 2005;48:352-4.
6. Pietrabissa A, Moretto C, Antonelli G, Morelli L, Marciano E, Mosca F. Thrombosis in the portal venous system after elective laparoscopic splenectomy. Surg Endosc 2004;18:1140-3.

7. Miniati DN, Padidar AM, Kee ST, Krummel TM, Mallory B. Portal vein thrombosis after laparoscopic splenectomy: an ongoing clinical challenge. JSLS 2005;9:335-8.
8. Valla DC, Condat B, Lebrec D. Spectrum of portal vein thrombosis in the West. J Gastroenterol Hepatol 2002; (Suppl 3):S224-7.
9. Stamou KM, Toutouzas KG, Kekis PB, Nakos S, Gafou A, Manouras A, et al. Prospective study of the incidence and risk factors of postsplenectomy thrombosis of the portal, mesenteric, and splenic veins. Arch Surg 2006;141:663-9.
10. Winslow ER, Brunt LM, Drebin JA, Soper NJ, Klinqensmith ME. Portal vein thrombosis after splenectomy. Am J Surg 2002;184: 631-6.
11. Hayes DM, Spurr CL, Hutaff LW, Sheets JA. Post-splenectomy thrombocytosis. Ann Intern Med 1963;58:259-67.
12. Broe PJ, Conley CL, Cameron JL. Thrombosis of the portal vein following splenectomy for myeloid metaplasia. Surg Gynecol Obstet 1981;152:488-92.
13. Ikeda M, Sekimoto M, Takiguchi S, Kubota M, Ikenaga M, Yamamoto H, et al. High incidence of thrombosis of the portal venous system after laparoscopic splenectomy: a prospective study with contrast-enhanced CT scan. Ann Surg 2005;241:208-16.
14. Eguchi A, Hashizume M, Kitano S, Tanoue K, Wada H, Sugimachi K. High rate of portal thrombosis after splenectomy in patients with esophageal varices and idiopathic portal hypertension. Arch Surg 1991;126:752-5.
15. de Cleva R, Herman P, Saad WA, Puqliese V, Zilberstein B, Rodriguess JJ, et al. Postoperative portal vein thrombosis in patients with hepatosplenic mansonic schistosomiasis: relationship with intraoperative portal pressure and flow. A prospective study. Hepatogastroenterology 2005;52: 1529-33.
16. Ikeda M, Sekimoto M, Takiguchi S, et al. Total splenic vein thrombosis after laparoscopic splenectomy: a possible candidate for treatment. Am J Surg 2007;193:21-5.
17. Poultsides GA, Lewis WC, Feld R, Walters DL, Cherry DA, Ruby ST. Portal vein thrombosis after laparoscopic colectomy: thrombolytic therapy via the superior mesenteric vein. Am Surg 2005;71:856-60.
18. Jakimowicz J, Stultiens G, Smulders F. Laparoscopic insufflation of the abdomen reduces portal venous flow. Surg Endosc 1998;12:129-32.
19. Takagi S. Hepatic and portal vein blood flow during carbon dioxide pneumoperitoneum for laparoscopic hepatectomy. Surg Endosc 1998;12:427-31.
20. Baixauli J, Delaney CP, Senagore AJ, et al. Portal vein thrombosis after laparoscopic sigmoid colectomy for diverticulitis: report of a case. Dis Colon Rectum 2003;46: 550-3.

OPEN ACCESS Freely available online

PLoS one

Dicer Is Required for Maintaining Adult Pancreas

Sumiyo Morita[1,2], Akemi Hara[3], Itaru Kojima[3], Takuro Horii[1], Mika Kimura[1,2], Tadahiro Kitamura[4], Takahiro Ochiya[5], Katsumi Nakanishi[6], Ryo Matoba[6], Kenichi Matsubara[6], Izuho Hatada[1]*

1 Laboratory of Genome Science, Biosignal Genome Resource Center, Institute for Molecular and Cellular Regulation, Gunma University, Showa-machi Maebashi, Japan, 2 Japan Health Sciences Foundation, Chuo, Tokyo, Japan, 3 Department of Molecular Medicine, Institute for Molecular and Cellular Regulation, Gunma University, Showa-machi Maebashi, Japan, 4 Metabolic Signal Research Center Laboratory of Metabolic Signal, Institute for Molecular and Cellular Regulation, Gunma University, Showa-machi Maebashi, Japan, 5 National Cancer Center Research Institute, Section for Studies on Metastasis, Tsukiji, Chuo-ku, Tokyo, Japan, 6 DNA Chip Research Inc., Suehirocho, Tsurumi-ku, Yokohama, Japan

Abstract

Dicer1, an essential component of RNA interference and the microRNA pathway, has many important roles in the morphogenesis of developing tissues. *Dicer1* null mice have been reported to die at E7.5; therefore it is impossible to study its function in adult tissues. We previously reported that *Dicer1*-hypomorphic mice, whose *Dicer1* expression was reduced to 20% in all tissues, were unexpectedly viable. Here we analyzed these mice to ascertain whether the down-regulation of *Dicer1* expression has any influence on adult tissues. Interestingly, all tissues of adult (8–10 week old) *Dicer1*-hypomorphic mice were histologically normal except for the pancreas, whose development was normal at the fetal and neonatal stages; however, morphologic abnormalities in *Dicer1*-hypomorphic mice were detected after 4 weeks of age. This suggested that *Dicer1* is important for maintaining the adult pancreas.

Citation: Morita S, Hara A, Kojima I, Horii T, Kimura M, et al. (2009) Dicer Is Required for Maintaining Adult Pancreas. PLoS ONE 4(1): e4212. doi:10.1371/journal.pone.0004212

Editor: Kerby Shedden, University of Michigan, United States of America

Received October 22, 2008; **Accepted** December 9, 2008; **Published** January 16, 2009

Funding: This work was supported in part by the Japan Health Sciences Foundation (S.M. is a fellowship holder from the Japan Health Sciences Foundation), grants from the Ministry of Education, Culture, Sports, Science and Technology of Japan (I.H. and I.K.), the Ministry of Health, Japan Health Sciences Foundation, Labor and Welfare of Japan (T.O. and I.H.) and a grant from the Realization of Regenerative Medicine (I.K.). The funders had no role in study design, data collection and analysis, decision to publish, or preparation of the manuscript.

Competing Interests: The authors have declared that no competing interests exist.

* E-mail: ihatada@showa.gunma-u.ac.jp

Introduction

MicroRNA (miRNA) is small (~22 nucleotides), non-coding RNA. Mature miRNA transcribed as long primary transcripts is processed to pre-miRNA in the nucleus by *Drosha/DGC8* [1], and then processed in the cytoplasm by *Dicer* [2]. MiRNA is further incorporated into the RNA-inducing silencing complex (RISC), which includes Argonaute [3] to regulate gene expression via post-transcriptional repression. Over the past few years, more than 400 miRNAs have been identified, but their function is largely unknown. Several miRNAs exhibit tissue-specific or developmental stage-specific expression [4,5], indicating that they have important roles in many biological processes.

Dicer1 encodes an RNaseIII endonuclease, a key enzyme that processes miRNA. It is broadly expressed in developing tissues, and several mutant alleles of *Dicer1* have been generated in mice. *Dicer1* seems to be critical in early development since loss of its function was lethal at embryonic day 7.5 [6]. Characterization of *Dicer1* hypomorphic mice showed that the gene is required for embryonic angiogenesis [7]. Conditional inactivation of *Dicer1* in the mouse limb bud mesenchyme [8], lung epithelium [9], epidermal hair follicle [10], and pancreas [11], T cell development and differentiation [12] led to the conclusion that *Dicer1*, which processes miRNA, is indispensable for the development and morphogenesis of these tissues.

We previously generated *Dicer1*-hypomorphic mice (homozygous *Dicer1*−/− mice) [13]. Complete loss of *Dicer1* in mice results in early embryonic death [6]; however, our *Dicer1*-hypomorphic mice were viable [13]. To study the function of *Dicer1* in the maintenance of homeostasis in adult tissues, we analyzed the adult tissues histologically and found abnormalities only in the pancreas. The phenotypes detected in the pancreas of *Dicer1*-hypomorphic mice might resemble the differentiation of endocrine precursor cells in adult pancreas.

The pancreas consists of three main tissue cell types: the endocrine cells (islet of Langerhans) which produce hormones such as insulin and glucagon; the exocrine acinar tissues which secrete digestive enzymes; and the branched duct. Numerous mechanisms that control the differentiation of endocrine and exocrine cells in the embryonic pancreas have been revealed [14], but how endocrine cells (especially insulin-producing β cells) are maintained in postnatal life has been controversial [15]. At E9.5, the endocrine cells of the pancreas arise from endocrine precursor cells, which express both glucagon and insulin and divide into distinct lineages such as glucagon or insulin-expressing cells. On the other hand, in the adult pancreas, it had been considered that there are no endocrine progenitor cells and that β cells are generated only by the replication of existing β cells, not from the differentiation of endocrine precursor cells (neogenesis) [16,17]. However, several studies suggested that β cell differentiation from endocrine precursor cells can occur in adults in the regenerating pancreas after a partial pancreatectomy or duct ligation [18,19,20,21]. In the regenerating pancreas, vigorous expansion of the β cell population was observed, and partial pancreatectomy and duct ligation has been a good model for regenerating endocrine cells. The phenotypes observed in *Dicer1*-hypomorphic

mice suggested that *Dicer1* regulates the endocrinal neogenesis in the adult pancreas. Previous study showed that *Dicer1* is indispensable for normal development of the pancreas [11]; however, its function in the adult pancreas had not been elucidated. Here we report that *Dicer1* also has important functions in the adult pancreas.

Results

Dicer1 expression was significantly reduced in all tissues of *Dicer1*-hypomorphic mice but histological abnormalities were only found in the pancreas

Dicer1-hypomophic mice (homozygous *Dicer1*−/− mice) showed a lower birth rate than expected by Mendelian rules [13]; however, they did not differ from their wild-type littermates in overall health. Although they showed slight growth retardation from 10 to 50 days of age, their body weight was similar to that of wild-type mice after 50 days of age (Fig. 1). A comparison of *Dicer1* expression in nine tissues of adult mice revealed a 70–85% reduction in the hypomorphic mice (Fig. 2). Although we analyzed more than 40 tissues (Table 1), histological examination revealed no abnormalities in any tissues except the pancreas (Fig. 3); thus we focused on the pancreas of *Dicer1*-hypomorphic mice.

Dicer1 could be involved in differentiation of endocrine cells in adult pancreas

In *Dicer1*-hypomorphic mice, the size of the pancreas in adults (8–10 weeks of age) was nearly identical to that in the wild-type mice; however, there were more small islets (Fig. 4). In some of these islets, the distribution of islet cells and staining of nuclei were irregular (Fig. 5A). The boundary of islets and ducts was not clearly defined in the pancreas (Fig. 5B). Immunohistochemical analysis revealed mostly normal staining of insulin and glucagon at 8–10 weeks of age; however, the number of ductal epithelial cells stained with insulin or glucagon was significantly increased (Fig. 5C-III, P = 0.0051). In some models of pancreatic regeneration including partial pancreatectomy, insulin or glucagon-stained cells are present in the ductal epithelium, which had led to the idea that some endocrine cells differentiate in the ducts [18,19,20,21]. Our observations in *Dicer1*-hypomorphic mice suggest that regeneration from the endocrine precursor cells took

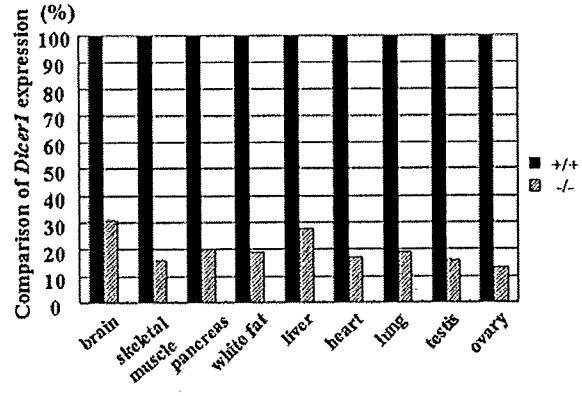

Figure 2. Comparison of *Dicer1* expression in nine tissues between wild-type (+/+) and *Dicer1*-hypomorphic (−/−) mice. The expression in the *Dicer1*-hypomorphic mice was normalized to that in the wild-type mice.
doi:10.1371/journal.pone.0004212.g002

place in adulthood. Next we conducted a histological examination of the markers Pdx-1 and Ki67. The population of ducts containing Pdx-1-positive cells was significantly increased (Fig. 5C-IV, P = 0.009). Pdx1-positive cells in the ducts are possibly the adult progenitor cells [22,23], and PDX-1 protein was detected in the pancreatic duct in adult rats after partial pancreatechtomy [21]. Surprisingly, abnormal staining of Ki67, which is a marker for proliferation of the cells, was detected in the pancreatic ducts in two of six *Dicer1*-hypomorphic mice (Fig. 5C-V). In some Ki-67-positive ducts, all the epithelial cells were stained. No such observations were found in wild-type mice.

Interestingly, cells morphologically different from either acinar or islet cells were observed in *Dicer1*-hypomorphic mice (Fig. 5D-I). Under a light microscope, some appeared to be syncytial multinucleated cells near the pancreatic duct and in acini. Numerous nuclei were distributed irregularly and were often clustered in the cells, which were all double-positive for insulin and glucagon (Fig. 5E). Cells double-positive for insulin and glucagon were significantly increased in *Dicer1*-hypomorphic mice compared to wild-type mice (Fig. 5D-II, P = 0.0019). In the exocrine portion of

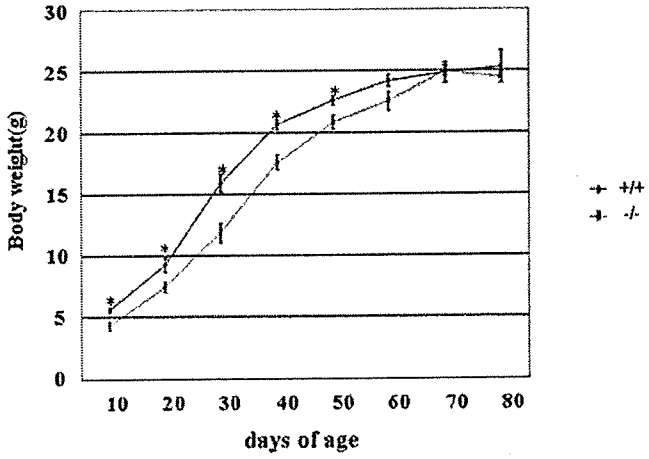

Figure 1. Body weight growth curves. Male wild-type (+/+) and *Dicer1*-hypomorphic (−/−) mice were measured to determine the change in body weight from 10 to 80 days of age. *, P<0.05. n = 8–10 per group.
doi:10.1371/journal.pone.0004212.g001

Table 1. The list of tissues with histological analysis (H&E assessment).

lung	testis	eye ball	trachea
heart	epididymis	harderian gland	esophagus
kidney	prostate	skeletal muscle	thyroid gland
pancreas	seminal vesicle	sciatic nerve	liver
tongue	coagulating gland	skin	cholecyst
stomach	bladder	breast bone	spleen
duodenum	adrenal	femur	
jejunum	pituitary gland	cerebrum	
ileum	submandibular gland	hippocampus	
cecum	parotid gland	thalamus	
colon	thymus	cerebellum	
rectum	cervical lymph node	spinal cord	

Histological analysis of these tissues was performed in wild-type (+/+) (n = 2) and *Dicer1*-hypomorphic (−/−) mice (n = 4).
doi:10.1371/journal.pone.0004212.t001

the pancreas of *Dicer1*-hypomorphic mice, most acini were morphologically normal, but some showed an irregular morphology (Fig. 5F). The shapes and position of the cells were irregular and the acinar structure was not organized. In normal acinar cells, zymogen granules are observed in the center of the acinus and the nucleus is located at its periphery.

We next investigated when the abnormal morphology appeared in the development of the pancreas in *Dicer1*-hypomorphic mice. For this purpose, a histological analysis was performed using E15.5 embryos, P1 mice, and 4-week-old mice. The pancreas of both wild-type and *Dicer1*-hypomorphic mice developed normally and endocrine and exocrine cells appeared morphologically normal at E15.5 and P1 (Fig. 6A, B); the same abnormalities observed in adult *Dicer1*-hypomorphic mice were detectable at 4 weeks of ages (Fig. 6C), although the number of abnormal cells was less than that found in adult *Dicer1*-hypomorphic mice. This suggested that the pancreas of *Dicer1*-hypomorphic mice developed normally after birth and abnormal cells appeared at around 4 weeks after birth, increasing with age.

Surprisingly, the observations found in *Dicer1*-hypomorphic mice were quite similar to the histological findings in transgenic mice expressing a truncated type II activin receptor [24]. Therefore, we next investigated the expression of the activin type II receptor in the pancreas of *Dicer1*-hypomorphic mice. Two related receptors, ActRIIA and ActRIIB, were initially identified as type II receptors for activin [25,26]. ActRIIA and ActRIIB have been reported to bind not only to activin [27], but also to other TGF-β family proteins, including BMP7 [28], GDF8 [29], Nodal [30], and GDF11 [31]. The precise role of the two activin receptors is still not clear. Real-time PCR analysis revealed that the expression of ActRIIA was slightly up-regulated in *Dicer1*-hypomorphic mice compared to wild-type mice, while the expression of ActRIIB did not differ (Fig. 7). Therefore, the abnormal morphology might be attributed to another signaling cascade.

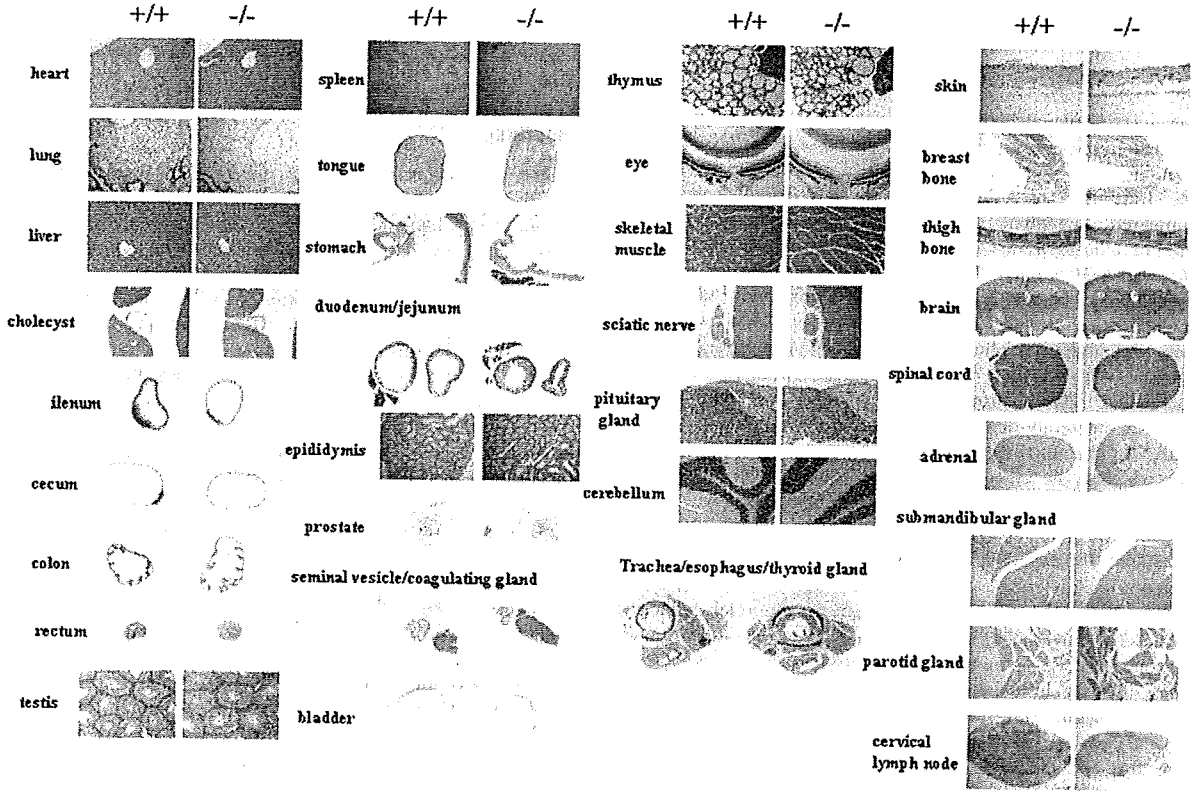

Figure 3. H&E-stained section of adult tissues of wild-type (+/+) (n = 2) and *Dicer1*-hypomorphic (−/−) mice (n = 4).
doi:10.1371/journal.pone.0004212.g003

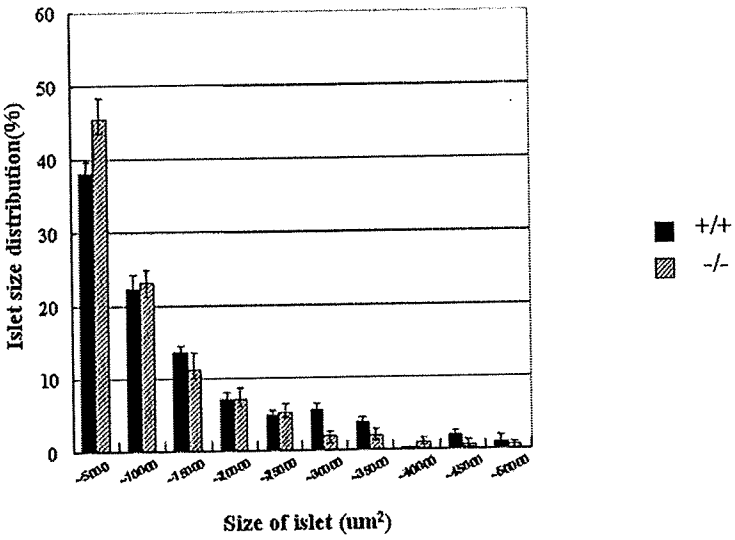

Figure 4. Comparison of the size of islets in wild-type and *Dicer1*-hypomorphic mice. The islets mass was measured in wild-type (blue bar) and *Dicer1*-hypomorphic mice (pink bar). The numbers of islets were examined in wild-type (n = 6) and *Dicer1*-hypomorphic (n = 6) mice, with six sections from each animal. The graph shows the percentage of islets in each size category.
doi:10.1371/journal.pone.0004212.g004

Detection of differential expressed miRNAs by microarray analysis

Because *Dicer1* is required for the processing of miRNAs, the reduction of *Dicer1* results in a decrease in miRNAs. To determine the differential expression of miRNAs in the pancreas of adult wild-type and *Dicer1*-hypomorphic mice, a miRNA microarray analysis was performed. The miRNAs of the pancreas of two wild-type and two *Dicer1*-hypomorphic mice were analyzed. Signals were very weak on hybridization with miRNA in the pancreas compared to other tissues; therefore a total of 83 miRNAs, which showed strong signals, were analyzed. Fig. 8 shows the change in the distribution of miRNA levels in *Dicer1*-hypomorphic mice compared to wild-type mice. Surprisingly, miRNA expression did not dramatically change in *Dicer1*-hypomorphic mice compared to the wild-type animals: however, 7% of miRNAs were down-regulated less than 0.5 fold. These miRNAs might function in maintaining the adult pancreas, but at present their relationship with the abnormal phenotype in *Dicer1*-hypomorphic mice is unclear. Why was only 7% of the miRNA expressed in pancreas attenuated? Dicer1 protein might catalyze processing of pre-miRNA differently dependent on the sequence when generating miRNA. The down-regulated miRNAs might be more difficult to process than the other miRNAs and thus significantly reduced *Dicer1* expression might affect their generation.

Glucose metabolism was normal in *Dicer1*-hypomorphic mice

The hypo-expression of *Dicer1* leads to abnormal endocrine cells, which might affect the function of the pancreas; therefore, we next investigated the metabolism of glucose in *Dicer1*-hypomorphic mice. Despite histological abnormalities in pancreatic islets, a glucose tolerance test showed that *Dicer1*-hypomorphic mice were able to clear glucose from the blood as efficiently as wild-type mice (Fig. 9A), and had insulin levels similar to wild-type mice (Fig. 9B). Despite no significant differences in the insulin content of serum after overnight fasting, *Dicer1*-hypomorphic mice showed a slightly reduced blood glucose level on fasting. *Dicer1*-hypomorphic mice were smaller than the wild-type mice before 50 days of age; therefore, we hypothesized that the growth hormone level affects fasting hypoglycemia. We checked the blood growth hormone level; however, we found no significant differences with wild-type mice (Fig. 9C). Thus, the growth hormone level is not responsible for fasting hypoglycemia in *Dicer1*-hypomorphic mice, probably due to an unknown mechanism involved in glucose metabolism in other tissues.

Discussion

Dicer, the enzyme that generates miRNAs, has been reported to have quite important roles in a variety of developmental processes. In our *Dicer1*-hypomorphic mice, histological analysis (H&E assessment) showed that the abnormalities were found only in the pancreas and not in other tissues. However, we could not exclude the possibility that there are more minute structural abnormalities not detected with the H&E assessment, or functional abnormlities. In this study, we focused on the pancreas. The pancreatic-specific knockout of *Dicer1* clarified that miRNA is required for the development of the pancreas in embryogenesis [11]. Our study suggested that *Dicer1* also has important functions in maintaining the adult pancreas.

Histological abnormalities such as the irregular distribution of islet cells, and deviations from the typical structure of the acinus, were found in endocrine and exocrine cells in the adult pancreas of *Dicer1*-hypomorphic mice, although none of these abnormalities were detected before 4 weeks of age. *Dicer1* is indispensable for normal pancreatic cell differentiation at embryogenesis [11]. The pancreas-specific *Dicer1* knockout mice survived until birth but died before P3. These mice showed gross defects in all pancreatic lineages, and the formation of exocrine cells and duct cells, especially endocrine cells, was greatly impaired. Given that miRNA most probably plays essential roles in the morphogenesis of many tissues in a developing embryo [7,8,9,10,12], the gross defects in all pancreatic lineages observed upon removal of *Dicer1* are not surprising. These mice died soon after birth; therefore, it is impossible to study the role *Dicer* may play in adult tissues.

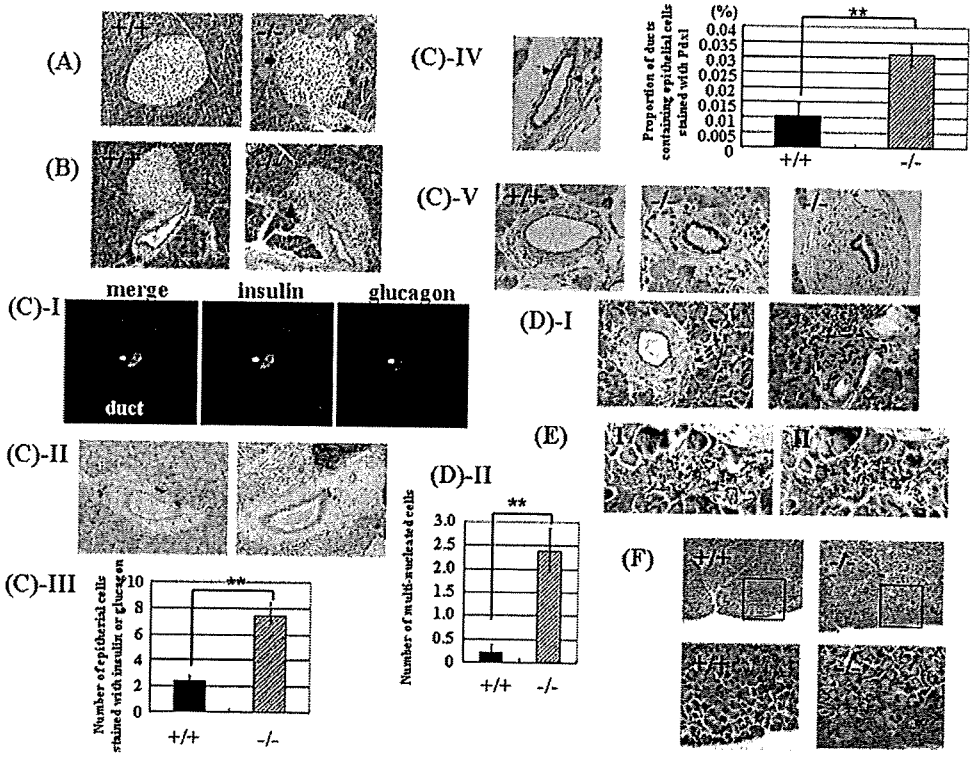

Figure 5. Pancreas morphology in adult (8–10 weeks of age) *Dicer1*-hypomorphic mice. A, B: Hematoxylin-eosin (H & E)-stained islets of the pancreas from an 8-week-old wild-type (+/+) mouse and *Dicer1*-hypomorphic (−/−) mice (*400). A: Arrows indicate an irregular distribution of islet cells. B: Arrowheads indicate that the boundary of islets and ducts was not clearly defined in the pancreas of *Dicer1*-hypomorphic mice. C: Immunohistochemistry of duct cells of *Dicer1*-hypomorphic mice. (I) Insulin (green) and glucagon (red) double-expressing cells were detected in the duct. (II) Insulin-positive cells (brown) and glucagon-positive cells (blue) were observed in the duct. (III) Comparison of the number of epithelial cells stained with both insulin and glucagon, only insulin, and only glucagon in wild-type and *Dicer1*-hypomorphic mice. These numbers were averaged from 6 animals, with six sections from each animal. **, P<0.01. (IV) Comparison of the proportion of ducts containing epithelial cells stained with Pdx1 in wild-type and *Dicer1*-hypomorphic mice. Arrowheads indicate the Pdx1-positive cells. *, P<0.01. (V) Abnormal staining of Ki67 was observed in the pancreas of *Dicer1*-hypomorphic mice. D: (I) H & E-stained multinuclear atypical cells in the pancreas of *Dicer1*-hypomorphic mice. The black dotted line indicates atypical multinuclear cells. (II) Comparison of the number of multi-nucleated cells in wild-type and *Dicer1*-hypomorphic mice. These numbers were averaged from 6 animals, with six sections from each animal. **, P<0.01. E: Immunohistochemistry of multinuclear atypical cells of adjacent sections of the pancreas of *Dicer1*-hypomorphic mice using anti-insulin (I) and anti-glucagon (II) antibodies. F: H & E-stained acinar cells. The rectangular areas outlined in the upper panels are magnified in the lower panels. An abnormal structure of exocrine cells was observed in the pancreas of *Dicer1*-hypomorphic mice.
doi:10.1371/journal.pone.0004212.g005

The pancreas of our *Dicer1*-hypomorphic mice developed normally and the reduced expression of *Dicer1* did not affect the development of the pancreas during embryogenesis or the neonatal stage. However, aberrant endocrine and exocrine cells could be detected after 4 weeks of age, and the number of abnormal regions seemed to increase with age. It is interesting that the developing pancreas during embryogenesis and the adult pancreas differ in sensitivity to the *Dicer1* level. In other words, the reduction in *Dicer1* only affects the maintaining of adult pancreas, not the normal development of the pancreas.

In addition, these observations, such as the increasing number of ductal epithelial cells stained positive for insulin, glucagon, and Pdx-1 in *Dicer1*-hypomorphic mice (Fig. 5D-III, IV), were also found in the regenerating pancreas [18,19,20,21], suggesting that the differentiation of endocrine precursor cells (neogenesis) occurred in the adult pancreas. Moreover, a quite intriguing observation was the existence of unknown abnormal multi-nucleated cells in the pancreas that expressed both glucagon and insulin. In the developing pancreas, endocrine precursor cells first appeared at E9, and these cells expressed both glucagon and insulin [32,33], then differentiated into insulin-producing cells or glucagon-producing cells. These cells in our adult *Dicer1*-hypomorphic mice resembled endocrine precursor cells in the fetal pancreas in terms of the expression of both glucagon and insulin. Therefore, *Dicer1* might have roles in regulating endocrine precursor cells in the adult pancreas.

The proliferation of duct cells is increased in the regenerating pancreas compared to the normal adult pancreas [20]. However, in some *Dicer1*-hypomorphic mice, abnormal proliferation of duct epithelial cells was observed (Fig. 5D-V). These features were not detected in wild-type mice and could be caused by the reduction in *Dicer1*.

Surprisingly, these histological observations in *Dicer1*-hypomorphic mice were quite similar to the histological findings in transgenic mice expressing the truncated type II activin receptor [24]. However, as our *Dicer1*-hypomorphic mice showed only a 1.2-fold increase in ActRIIA in the pancreas, ActRIIA might not cause the abnormal phenotype.

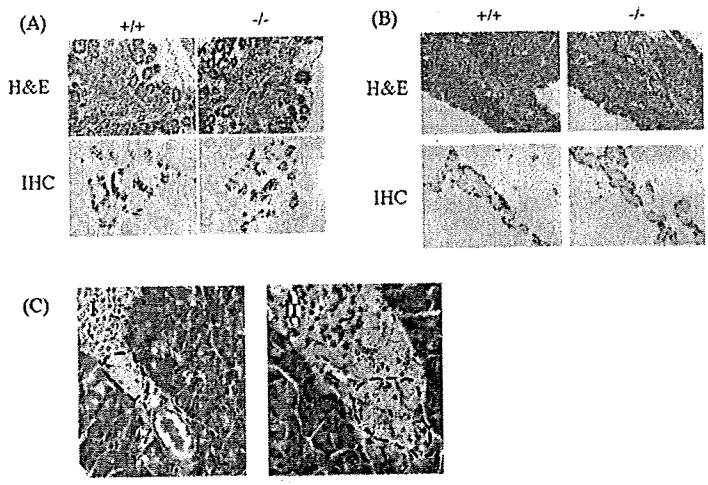

Figure 6. Histological and immunohistochemical analysis of the pancreas at E15.5 (A) and P1 (B) of wild-type and *Dicer1*-hypomorphic mice. *Dicer1*-hypomorphic mice show normal insulin (brown) and glucagon (blue) staining at E15.5 and P1. C: Histological abnormalities found in the pancreas of 4-week-old *Dicer1*-hypomorphic mice. (I) The endocrinal distribution was slightly irregular. The dotted line indicates the abnormal region of the islet. (II) Multi-nucleated cells were observed. The dotted line indicates multi-nucleated cells, which were also found in the pancreas of adult *Dicer1*-hypomorphic mice.
doi:10.1371/journal.pone.0004212.g006

Because *Dicer1* has a key role in generating a large number of miRNAs, its removal results in a significant decrease in miRNAs. In the pancreas of our *Dicer1*-hypomorphic mice, the expression levels of miRNA changed slightly compared to wild-type level which is why the mice could survive. A complete loss of *Dicer* in mice results in early embryonic death. A large number of genes control the development or maintenance of the pancreas, and these genes might be a potential target of miRNAs. Even a slight change in miRNA expression might affect the gene expression, leading to the abnormal morphology in *Dicer1*-hypomorphic mice. Further exploration is necessary to investigate the relation between these genes and miRNA in the pancreas.

Our results suggest that *Dicer1* functions in the adult pancreas and also raise the possibility that *Dicer1* regulates the differentiation of endocrine precursor cells there. Further analysis is necessary to understand the mechanism behind the maintenance of each cell type in the adult pancreas, especially β cells.

Materials and Methods

Gene targeting and mice

We generated *Dicer1*-deficient mice from an ES cell (RFF266), which was obtained from Bay Genomics [34], carrying a gene trap insertion between exon 22 and exon 23, resulting in disruption of the second RNaseIII domain and loss of the double-stranded RNA-binding domain. A gene trap vector called pGT1Lxf, which has a splicing acceptor, was used to make this ES cell. Targeted clones were injected into blastocysts to generate chimeras. Five chimeras were generated and backcrossed with

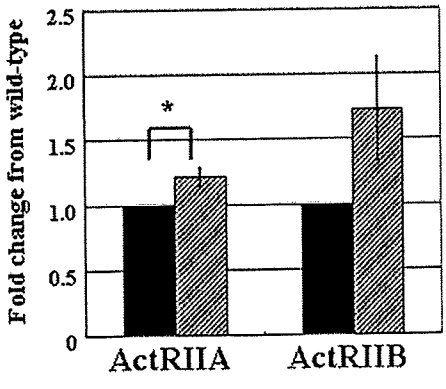

Figure 7. Analysis of ActRIIA and ActRIIB expression. Data are expressed relative (n-fold) to the wild-type pancreas and correspond to the means and standard errors for three independent experiments performed in triplicate. *, $P<0.05$. wild-type n = 9, *Dicer1*-hypomorphic mice n = 9.
doi:10.1371/journal.pone.0004212.g007

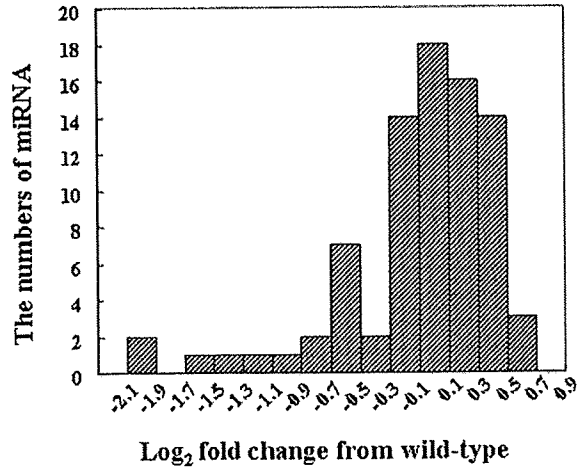

Figure 8. The distribution of changes in miRNA levels in *Dicer1*-hypomorphic mice compared to wild-type mice.
doi:10.1371/journal.pone.0004212.g008

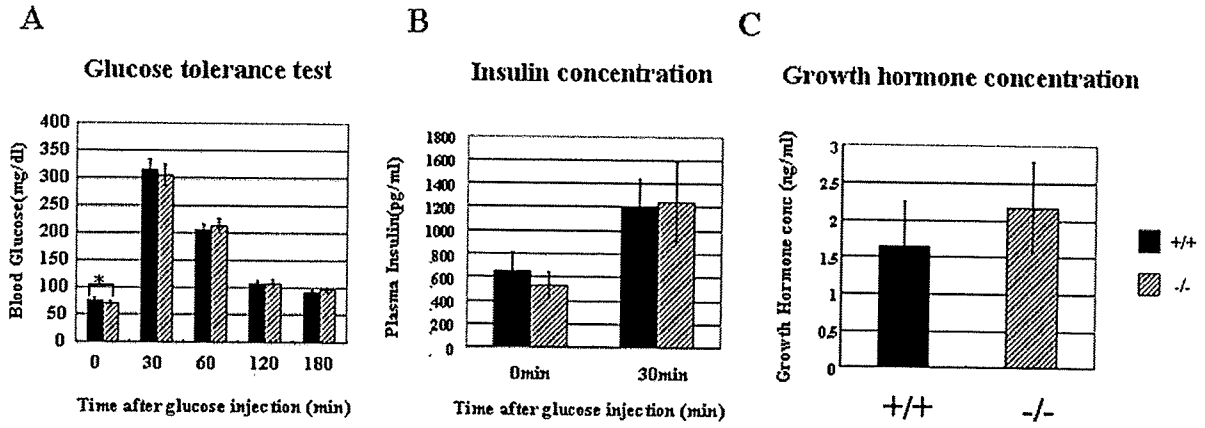

Figure 9. Glucose metabolism and growth hormone levels in wild-type and *Dicer1*-hypomorphic mice. A: Glucose tolerance test. Fasted 8-week-old mice received an intraperitoneal injection of glucose (2 mg/g body weight). B: Insulin concentration. Plasma insulin was measured before and after the intraperitoneal glucose injection. C: Growth hormone concentration. Plasma growth hormone concentrations were measured in wild-type and *Dicer1*-hypomorphic mice. A, B: Values are expressed as the means±S.D. (n = 10 per group).*, $P<0.05$.
doi:10.1371/journal.pone.0004212.g009

C57BL/6 mice. *Dicer1* heterozygous mice were backcrossed with C57BL/6 mice for 12 generations. All animal experiments were approved by the Animal Research Ethics Board at the Gunma University.

Histochemistry and immunohistochemistry

Tissues and embryos were fixed overnight in formalin at 4°C and embedded in paraffin. Standard techniques were used for the embedding, sectioning and staining of tissues. Sections were cut at 5 μm. Immunohistochemistry was performed as follows: The slides were dewaxed and washed in PBS, and blocked in 1% BSA for 30 min. They were then incubated with primary antibodies overnight at 4°C in PBS containing 1% BSA, washed in PBS, and incubated with the appropriate secondary antibodies for 1 hour at room temperature. The slides were washed in PBS and mounted with Pristine Mount (Parma) with DAPI. The primary antibodies used were rabbit anti-glucagon (1:200, DAKO) and guinea pig anti-insulin (1:200, DAKO), rabbit Ki67 monoclonal antibody (Lab Vision), and Pdx1 (a gift from Christopher V. Wright (Vanderbilt University, Nashville)). The secondary antibodies were conjugated to rodamin (1:200, Jackson) and Alexa 488 (1:200, Molecular Probes). The slides were examined with a Nikon ECLIPSC TE300 and images were obtained with a LEICA DFC400 camera.

Measurement of islet area

ß-cell mass was measured using Image J software (NIH). Islet numbers and areas were averaged from 6 animals, with six sections from each animal, 250 μm apart.

RNA extraction and quantitative RT-PCR

Total RNA was prepared from isolated tissues using the RNeasy mini kit (Qiagen) with a modified protocol to purify total RNA containing miRNA from animal tissues. Differential gene expression was confirmed using the SYBR Premix Ex Taq (TAKARA) in accord with the manufacturer's instructions. The reaction was performed using the SYBER Green program on an ABI PRISM 7700 sequence detector system (Applied Biosystems). The expression of mRNA was normalized to that of GAPDH mRNA.

Primer sequences were as follows, ActRIIA: 5′-AGCGGAG-CTGACAGTGATTT-3′, 5′-CATACACGCACAACACACCA-3′ ActRIIB: 5′-TGGACATCCATGAGGTGAGA-3′, 5′-CAGCAG-CTGTAGTGGCTTCA-3′

miRNA microarray

Small RNAs were labeled with a miRNA labeling Reagent & Hybridization Kit (Agilent) based on the manufacturer's instructions. The Cy3-labeled RNA molecules were hybridized with a Mouse miRNA microarray (Agilent), consisting of control probes, mismatch probes, and 567 capture probes as registered and annotated in Sanger miRBase v10.1. A DNA MicroArray Scanner (Agilent) was used to scan images. The scanned images were analyzed with Agilent Feature Extractin Ver.9.5.3 (Agilent). Data were normalized globally per array. The net intensity values were normalized to per-chip median values.

Glucose tolerance test and insulin concentration

After overnight fasting, 2 mg/g (body weight) of glucose was administered intraperitoneally. Blood samples were drawn intraperitoneally from the tail at different times, and the blood glucose concentration was measured with an automatic blood glucose meter, Freestyle Freedom (NIPRO). Whole blood was collected and centrifuged, and the plasma was stored at −80°C. The insulin concentration was measured with an insulin measurement kit (Morinaga) in accordance with the manufacturer's instructions.

Growth hormone measurements

Growth hormone concentrations of wild-type and *Dicer1*-hypomorphic mice were measured with a rat/mouse growth hormone ELISA kit (LINCO Research).

Data analysis

Data were analyzed by the one-sample t-test and independent samples t-test. Data are the means±S.D.

Acknowledgments

We thank the Mutant Mouse Regional Resource Center (MMRRC) for providing RRF266 cells.

Author Contributions

Conceived and designed the experiments: SM IH. Performed the experiments: SM AH TH MK TK KN RM. Analyzed the data: SM IK TK TO KM. Contributed reagents/materials/analysis tools: SM. Wrote the paper: SM.

References

1. Gregory RI, Yan KP, Amuthan G, Chendrimada T, Doratotaij B, et al. (2004) The microprocessor complex mediates the genesis of microRNAs. Nature 432: 235–240.
2. Bernstein E, Caudy AA, Hammond SM, Hannon GJ (2001) Role for a bidentate ribonuclease in the initiation step of RNA interference. Nature 409: 363–366.
3. Hammond SM, Boettcher S, Caudy AA, Kobayashi R, Hannon GJ (2001) Argonaute2, a link between genetic and biochemical analyses of RNAi. Science 293: 1146–1150.
4. Lagos-Quintana M, Rauhut R, Yalcin A, Meyer J, Lendeckel W, Tuschl T (2002) Identification of microRNA from mouse. Current Biology 12: 735–739.
5. Wienholds E, Kloosterman WP, Misaka E, Alvarez-Saavedra E, Berezikov E, et al. (2005) MicroRNA expression in zebrafish embryonic development. Science 309: 310–311.
6. Bernstein E, Kim SY, Carmell MA, Murchison EP, Alcorn H, et al. (2003) Dicer is essential for mouse development. Nat Genet 35: 215–217.
7. Yang WY, Yang DD, Songqing N, Sandusky GE, Zhang Q, et al. (2005) Dicer is required for embryonic angiogenesis during mouse development. J Biol Chem 280: 9330–9335.
8. Harfe BD, McManus MT, Mansfield JH, Hornstein E, Tabin CJ (2005) The RNaseIII enzyme Dicer is required for morphogenesis but not patterning of the vertebrate limb. Proc Natl Acad Sci USA 102: 10898–10903.
9. Harris KS, Zhang Z, McManus MT, Harfe BD, Sun X (2006) Dicer function is essential for lung epithelium morphogenesis. Proc Natl Acad Sci USA 103: 2208–2213.
10. Andl T, Murchison EP, Liu F, Zhang Y, Yunta-Gonzalez M, et al. (2006) The miRNA-processing enzyme Dicer is essential for morphogenesis and maintenance of hair follicles. Current Biology 16: 1041–1046.
11. Lynn FC, Skewes-Cox BAP, Kosaka Y, McManus MT, Harfe BD, et al. (2007) MicroRNA expression is required for pancreatic islet cell genesis in the mouse. Diabetes 56: 2938–2945.
12. Cobb BS, Nesterova TB, Thompson E, Hertweck A, O'Connor E, et al. (2005) T cell lineage choice and differentiation in the absence of the RNase III enzyme Dicer. J Exp Med 20: 1367–1373.
13. Fukasawa M, Morita S, Kimura M, Horii T, Ochiya T, et al. (2006) Genomic imprinting in Dicer1-hypomorphic mice. Cytogenet Genome Res 113: 138–143.
14. Habener JF, Kemp DM, Thomas MK (2005) Minireview: Transcriptional regulation in pancreatic development. Endocrinology 146: 1025–1034.
15. Ackermann AM, Gannon M (2007) Molecular regulation of pancreatic β-cell mass development, maintenance, and expansion. J Mol Endo 38: 193–206.
16. Dor Y, Brown J, Martinez OI, Melton DA (2004) Adult pancreatic beta-cells are formed by self-duplication rather than stem-cell differentiation. Nature 429: 41–46.
17. Teta M, Rankin MM, Long SY, Stein GM, Kushner JA (2007) Growth and regeneration of adult β cells dose not involve specialized progenitors. Dev Cell 12: 817–829.
18. Bonner-Weir S, Baxter LA, Schuppin GT, Smith FE (1993) A second pathway for regenerating of adult exocrine and endocrine pancreas. A possible recapitulation of embryonic development. Diabetes 42: 1715–1720.
19. Bertelli E, Bendayan M (1997) Intermediate endocrine-acinar pancreatic cells in duct ligation conditions. Am J Physiol Cell Physiol 273: C1641–C1649.
20. Bonner-Weir S, Toschi E, Inada A, Reits P, Fonseca SY, et al. (2004) The pancreatic ductal epithelium serves as apotential pool of progenitor cells. Pediatric Diabetes 5: 16–22.
21. Xu X, D'Hoker J, Stange G, Bonne S, De Leu N, et al. (2008) β cells can be generated from endogenous progenitors in injured adult mouse pancreas. Cell 132: 197–207.
22. Kritzik MR, Jones E, Chen Z, Krakowski M, Krahl T, et al. (1999) Pdx-1 and Msx-2 expression in the regenerating and developing pancreas. J Endocrinol 163: 523–530.
23. Song SY, Gannon M, Wahington MK, Scoggins CR, Meszoely IM, et al. (1999) Pdx-1 expressing pancreatic epithelium and islet neogenesis in transgenic mice overexpressing transforming growth factor alpha. Gastroenterology 117: 1416–1426.
24. Shiozaki S, Tajima T, Zhang YQ, Furukawa M, Nakazato Y, et al. (1999) Impaired differentiation of endocrine cells of pancreas in transgenic mouse expressing the truncated type II activin receptor. Biochimica et Biophysica Acta 1450: 1–11.
25. Attisano L, Wrana JL, Cheifetz S, Massague J (1992) Novel activin receptors: dinsinct genes and alternative mRNA splicing generate a repertoire of serine/threonine kinase receptors. Cell 68: 97–108.
26. Mathews LS (1994) Activin receptors and cellular signaling by the receptor serine kinase family. Endocr Rev 15: 310–325.
27. Attisano L, Carcamo J, Ventura F, Weis FM, Massague J, et al. (1993) Identificatin of human activin and TGF beta type I receptors that form heteromeric kinase complexes with type II receptors. Cell 75: 671–680.
28. Yamashita H, Ten Dijke P, Huylebroeck D, Sampath TK, Andries M, et al. (1995) Osteogenic protein-1 binds to activin type II receptors and induce certain activin-like effectors. J Cell Biol 130: 217–226.
29. Lee SJ, McPherron AC (2001) Regulation of myostain activity and muscle growth. Proc Natl Acad Sci USA 98: 9306–9311.
30. Yeo C, Whitman M (2001) Nodal signals to Smads through Cripto-dependent and Cripto-independent mechanisms. Mol Cell 7: 949–957.
31. Oh SP, Yeo CY, Lee Y, Schrewe H, Whitman M, et al. (2002) Activin type IIA and type IIB receptors mediate Gdf11 signaling in axial vertebral patterning. Gene Dev 16: 2749–2754.
32. Gittes GK, Rutter WJ (1992) Onset of cell-specific gene expression in the developing mouse pancreas. Proc Natl Acad Sci USA 89: 1128–1132.
33. Teitelman G, Alpert S, Polak JM, Martinez A, Hanahan D (1993) Precursor cells of mouse endocrine pancreas coexpress insulin, glucagon and the neuronal proteins tyrosine hydroxylase and neuropeptide Y, but not pancreatic polypeptide. Development 118: 1031–1039.
34. Stryke D, Kawamoto M, Huang CC, Johns SJ, King LA (2003) BayGenomics: a resorce of insertional mutations in mouse embryonic stem cells. Nucleic Acids Res 31: 278–281.

doi:10.1111/j.1440-1746.2008.05496.x

HEPATOLOGY

Rapid hepatic fate specification of adipose-derived stem cells and their therapeutic potential for liver failure

Agnieszka Banas,* Takumi Teratani,* Yusuke Yamamoto,*,† Makoto Tokuhara,‡ Fumitaka Takeshita,* Mitsuhiko Osaki,* Takashi Kato,† Hitoshi Okochi‡ and Takahiro Ochiya*

*Section for Studies on Metastasis, National Cancer Center Research Institute, Chuo-ku, †Department of Biology, School of Education, Waseda University, Shinjuku-ku, and ‡Department of Surgery, International Medical Center of Japan, Shinjuku, Tokyo, Japan

Key words
adipose, differentiation, hepatocyte, liver regeneration, mesenchymal stem cell.

Accepted for publication 13 April 2008.

Correspondence
Dr Takahiro Ochiya, Section for Studies on Metastasis, National Cancer Center Research Institute, 1-1, Tsukiji 5-chome, Chuo-ku, Tokyo 104-0045, Japan. Email: tochiya@ncc.go.jp

Abstract

Background and Aim: Multipotential mesenchymal stem cells (MSC), present in many organs and tissues, represent an attractive tool for the establishment of a successful stem cell-based therapy in the field of regeneration medicine. Adipose tissue mesenchymal stem cells (AT-MSC), known as adipose-derived stem cells (ASC) are especially attractive in the context of future clinical applications because of their high accessibility and minimal invasiveness during the procedure to obtain them. The goal of the present study was to induce human ASC into functional hepatocytes *in vitro* within a very short period of time and to check their therapeutic potential *in vivo*.

Methods: *In vitro* generated ASC-derived hepatocytes were checked for hepatocyte-specific markers and functions. Afterwards, they were transplanted into nude mice with liver injury. Twenty-four hours after transplantation, biochemical parameters were evaluated in blood serum.

Results: We have shown here that ASC can be differentiated into hepatocytes within 13 days and can reach the functional properties of primary human hepatocytes. After transplantation into mice with acute liver failure, ASC-derived hepatocytes can restore such liver functions as ammonia and purine metabolism. Markers of liver injury, alanine aminotransferase, aspartate aminotransferase, as well as ammonia, were decreased after ASC-derived hepatocyte transplantation.

Conclusions: Our data highlight the properties of ASC as having a special affinity for hepatocyte differentiation *in vitro* and liver regeneration *in vivo*. Thus, ASC may be a superior choice for the establishment of a therapy for injured liver.

Introduction

The liver is exposed to many factors such as drugs, xenobiotics and viruses, which cause chronic hepatitis and liver cirrhosis. In most cases these lead to hepatocellular carcinoma and finally to organ failure, where there is chronic inflammation, fibrosis and no longer any regeneration ability.[1]

At present, liver transplantation is the only effective treatment for severe liver injuries. However, because of organ rejection and lack of donors, alternative strategies are urgently needed.

Human primary hepatocytes are commercially available; however, maintaining them in *in vitro* culture is very difficult, if not nearly impossible. After a few days of *in vitro* culturing they lose their functions. Additionally, their usage does not solve the problem of rejection. These factors limit their experimental applications and exclude their clinical usage.

In the last few years, extrahepatic cell populations with the potential to impact liver diseases have been discovered. The potential candidate stem cells for therapy of an injured liver are mesenchymal stem cells (MSC), which can be obtained from different sources such as bone marrow (BM),[2] umbilical cord blood (UCB),[3] amniotic fluid (AF),[4] scalp tissue,[5] placenta,[6] or adipose tissue (AT)[7,8] of the human body. These cells reveal a multipotentiality and semi-infinite proliferation ability. The hepatogenic differentiation capacity of MSC has been confirmed in many independent studies on BM-MSC,[9–14] UCB-MSC,[15–16] and adipose-derived stem cells (ASC).[17–19] The possibility for their future application in the therapy of liver diseases is very promising. MSC can easily be obtained from a patient's own tissues, isolated *ex vivo*, expanded, differentiated toward hepatocytes, and transplanted back into the patient in the form of either undifferentiated MSC or MSC-derived hepatocytes. Such a possibility sidesteps the limits regarding ethical issues and immunocompatibility problems. Importantly, MSC represent an advantageous cell type for allogenic transplantation as well, because they are immuno-privileged with low major histocompatibility complex (MHC) I (histocompatibility

Journal of Gastroenterology and Hepatology 24 (2009) 70–77

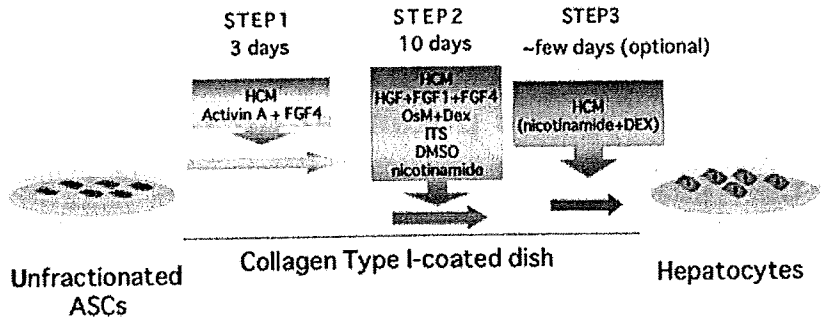

Figure 1 Improved and modified hepatogenic induction strategy. At present, approximately 2 weeks are required to induce hepatogenic characteristics in adipose-derived stem cells (ASC). Unfractionated ASC were plated on collagen type I-coated dishes and were treated with Activin A and FGF4 at step 1, followed by step 2, treatment with hepatocyte growth factor (HGF), fibroblast growth factor (FGF)1, FGF4, oncostatin M (OsM), dexamethasone, insulin-transferrin-selenium (ITS), dimethyl sulfoxide (DMSO), and nicotinamide. At this point, cells may be maintained a few days in hepatocyte culture medium (HCM) alone (or optionally supplemented with 10^{-8} mol/L dexamethasone and 0.05 mmol/L nicotinamide). MSC, mesenchymal stem cells.

lymphocyte antigen [HLA I]) and no MHC II (HLA II) expression, therefore reducing the risk of allogenic transplant rejection.[20–27]

Currently, attention is being given to adipose tissue (AT) as a source of MSC for regenerative medicine. From adipose tissue, a sufficient number of stem cells for a stem cell-based therapy may be obtained without invasiveness or damage to a patient's health. We have already demonstrated that human ASC have the ability to give rise to hepatocyte-like cells and that CD105 is a candidate mesenchymal stem cell marker.[19] However, this *in vitro* differentiation method is not applicable to a practical, clinical use, as more than 1 month is required to induce ASC into cells with hepatic functions.

In the present study, we evaluate the therapeutic potential of ASC-derived hepatocyte-like cells after transplantation into mice with liver injury. Clinical applications in the future would require a special approach, such as shortening as much as possible *ex vivo* manipulations, including cultivation and direct hepatic fate. Therefore, we improved and modified our hepatocyte differentiation strategy, based on the current knowledge on *in vivo* mouse fetal liver development. At present, a period as short as 13 days is required and that strategy is enriched by pretreatment with Activin A (PeproTech, EC, London, UK) and fibroblast growth factor (FGF)4 (PeproTech) (one of the factors secreted by septum transversum mesenchyme (STM) and cardiogenic mesoderm at the early stage of endoderm development *in vivo*). Additionally, we reorganized the content of the growth factor cocktail and enriched it with the addition of dimethyl sulfoxide (DMSO), nicotinamide and insulin-transferrin-selenium. Using the present protocol, we obtained functional hepatocyte-like cells in a much shorter period of time. Finally, we transplanted ASC-derived hepatocyte-like cells into immunodeficient mice with liver injury/non-severe acute liver injury. Our results showed a significant decrease of ammonia, aspartate aminotransferase (AST), alanine aminotransferase (ALT), and uric acid (UA) in the blood plasma of mice after ASC-derived hepatocyte-like cell transplantation. The results show a very important step towards future establishment of an alternative and successful therapy for liver disease.

Methods

Isolation and culturing of ASC

Adipose-derived stem cells were derived from abdominal subcutaneous adipose tissue, which was obtained from two female gastric cancer patients (Donor #1 [36 years old] and Donor #2 [45 years old]), undergoing gastrectomy at the International Medical Center of Japan, Tokyo. The hospital's committee of ethics approved this study, and informed consent was obtained from both patients. Adipose tissue was processed as previously described.[19] For *in vitro* differentiation, the cells (ASC062801, ASC012202, ASC0025) obtained from DS Pharma Biomedical Co., Osaka, Japan) were also analyzed.

Hepatic differentiation

At passage five to 10, the cells were plated on collagen type I-coated dishes at a concentration of $3.0–4.0 \times 10^4$ cells/cm^2 (Fig. 1). When the cells reached confluency, hepatogenic induction was carried out over a period of 2 weeks. First, the cells were treated for 3 days with DMEM (GibcoBRL, Tokyo, Japan) (serum free) supplemented with 20 ng/mL Activin A and 20 ng/mL FGF4 (PeproTech EC, London, UK). Afterwards, the cells were cultured for 10 days in a hepatocyte culture medium (HCM), containing 5 μg/mL transferrin, 10^{-6} mol/L hydrocortisone-21-hemisuccinate, 0.5 mg/mL bovine serum albumin, 2 mmol/L ascorbic acid, 20 ng/mL epidermal growth factor, 5 μg/mL insulin, 50 μg/mL gentamicin (Cambrex Corp., Walkersville, MD, USA) and supplemented with 150 ng/mL hepatocyte growth factor (HGF), 100 ng/mL FGF1, 25 ng/mL FGF4, 30 ng/mL oncostatin M (OsM; PeproTech), (2×10^{-5} mol/L) dexamethasone (Dex; Sigma, Tokyo, Japan), 1 × insulin-transferrin-selenium (ITS; Gibco), 0.05 mmol/L nicotinamide (Sigma), and 0.1% DMSO (Sigma). For the next few days, the cells were maintained with HCM alone. For *in vivo* transplantation, hepatocyte-like cells from two donors (#1 and #2) were harvested by treatment with a 0.05% collagenase/1000 U/mL dispase solution for 3–5 min, dissolved in

PBS (–) and injected intravenously into mice with liver injury caused by CCl_4 injection.

Quantitative real-time PCR

In order to confirm the regulation of the hepatocyte-specific genes in ASC-derived hepatocytes, we performed real-time polymerase chain reaction (PCR) for albumin (ALB) and tryptophan 2,3-dioxygenase (TDO2), with glyceraldehyde-3-phosphate dehydrogenase (GAPDH) as a reference gene. After retro-transcription, cDNA was subjected to real-time PCR by using Platinum Quantitative PCR Super Mix-UDG (Invitrogen, Tokyo, Japan) and specific primers for ALB (NM_000477): F:GTCACCAAATG CTGCACAGA, R:ACGAGCTCAACAAGTGCAGT for TDO2 (NM_005651): F:GTGTGCATGGTGCACAGAAT, R:GGGTT CATCTTCGGTATCCA, for FOXA2 (NM_021784): F:GGGA GCGGTGAAGATGGAAG, R:TGCCAGCGCCCACGTA and for GAPDH (NG_007073): F:GAAGGTGAAGGTCGGAGT, and R:GAAGATGGTGATGGGATTTC, based on the human genome database. The PCR conditions were as follows: denaturation at 95°C for 30 s, annealing at 56°C or 60°C for 30 s, and extension at 72°C for 30 s for up to 45 cycles. Real-time PCR was carried out by using the Applied Biosystems (Tokyo, Japan) PRISM 7700 Sequence Detection System.

Immunofluorescence

Cells were fixed in 4% formaldehyde for 10 min, followed by incubation with Protein Block (DakoCytomation, Carpinteria, CA, USA) for 30 min. ASC-derived hepatocytes were analyzed by immunohistochemistry using monoclonal anti-human specific albumin ALB (clone HAS-11, 1:250; Sigma) antibody overnight at 4°C. The Alexa Fluor 488 (green, 1:1000)-conjugated secondary antibody (Invitrogen, Tokyo, Japan) was applied for 30 min. Nuclei staining was performed using 4,6-diamidino-2-phenylindole (DAPI; Vector Laboratories, Burlingame, CA, USA).

Albumin production

Albumin production was evaluated by enzyme linked immunosorbent assay (ELISA, E80-129; Bethyl Laboratories, Montgomery, TX, USA). The antibody is human specific and does not cross-react with mouse, rat, bovine, goat, and pig albumin. Briefly, the supernatant during hepatogenic induction was collected every 3 days at days 3, 6 and 9, and ELISA assay was performed. Data are reported as the mean ± SD and were analyzed by Student's *t*-test, $n = 3$ ($^*P < 0.05$).

ASC-derived hepatocyte transplantation into mice with CCl_4-induced injury

Animal studies were carried out in compliance with the guidelines of the Institute for Laboratory Animal Research, National Cancer Center Research Institute. Six-week-old female BALB/c nude mice (CLEA Japan Inc., Tokyo, Japan) were used. An acute liver failure model was produced by giving one dose of CCl_4. At day 0, mice underwent i.p. injection of 100 μL/20 g bodyweight of olive oil containing 10 μL CCl_4. At day 1, mice underwent transplantation of ASC-derived hepatocyte-like cells (Donor #1 ($n = 4$), or Donor #2 ($n = 4$) at a concentration of 1.5×10^6 cells per mouse (0.2 mL cell suspension was injected through the tail vein). As a control, non-transplanted CCl_4-treated mice ($n = 3$) and non-transplanted CCl_4-non-treated (olive oil) ($n = 3$) mice were used. Twenty-four hours after transplantation, blood serum was collected and evaluated for biochemical parameters, such as AST, ALT, UA and ammonia concentration levels.

Assessment of liver functions

Blood samples were obtained from each mouse, centrifuged for 20 min at 400 *g* and serum was collected. Serum samples were tested for ammonia concentration level by using the Ammonia Test-Wako (Wako Pure Chemicals, Tokyo, Japan). The concentration of markers of liver injury such as ALT, AST and UA was analyzed by using a FUJIFILM DRI-CHEM 3500 machine and FUJI DRI-CHEM Slides for ALT/ALT-PIII, AST/AST-PIII, and UA-PIII, respectively (Fujifilm Co., Tokyo, Japan).

Statistical analysis

The results are given as the mean ± SD. Statistical analyses were conducted using either the variance with the Bonferroni correction for multiple comparisons or the Student's *t*-test. The statistical analysis of quantitative relative expression was evaluated by using the Pair Wise Fixed Reallocation Randomization Test©, Relative Expression Software Tool-XL = REST-XL© (http://www.gene-quantification.info/). A P value < 0.05 was considered significant.

Results

Hepatic fate specification of ASC

A direct fate hepatic specification (Fig. 1) was performed within 13 days. After that, ASC-derived hepatocyte-like cells could be maintained for a few days in HCM alone (optionally supplemented with Dex 10^{-8} mol/L and nicotinamide 0.05 mmol/L). After 3 days of pretreatment with FGF4 and Activin A, ASC expressed FOXA2 (Fig. 2a), the expression of which was decreased at day 6 of the induction system (3 days of pretreatment with FGF4 and Activin A, followed by 3 days of treatment with a cocktail containing HGF, FGF1, FGF4, OsM, Dex, ITS, DMSO and nicotinamide) (Fig. 2a). FOXA2, so-called hepatocyte nuclear factor 3β (HNF-3β) is an essential transcription factor for endoderm specification as well as hepatogenic fate. Similarly, ALB (hepatocyte-specific protein) and TDO2 (hepatocyte-specific enzyme, expressed by mature hepatocytes) were also detected by quantitative PCR at day 3 and their expression increased at day 6 of the induction system (Fig. 2a). The representative morphology of the ASC-derived hepatocyte-like cells of either a cancer patient's ASC or from the commercialized cells at the 13th day of induction is shown in Figure 2b. Importantly, 24 h of incubation with our new cocktail (Step II) alone is enough to dramatically influence the morphology of ASC (Donor #2) from fibroblast to epithelial (Fig. 3a). The pretreatment with Activin A and FGF4, however, is very important, because it induces the endodermal fate and alters further morphological changes and maturation of hepatocyte-like cells. As shown